Bull. Ind. Soc. Earth. Tech., Paper No.357, Vol.33. No.2, June 1996, pp 195-213

NONLINEAR SEISMIC RESPONSE OF REINFORCED CONCRETE STACK-LIKE STRUCTURES

Manoj K. Maiti* and Alok Goyal**
Department of Civil Engineering
Indian Institute of Technology
Powai, Bombay 400076, INDIA

ABSTRACT

A reliable technique for analyzing the inelastic dynamic response of reinforced concrete stack-like structures is presented in this paper. The deformed configuration of stack is idealized as an assemblage of beam elements and the element matrices are evaluated utilizing the actual stress-strain relationships of concrete and reinforcing steel. An adaptive time-step reduction scheme is suggested for efficient evaluation of the inelastic response. An example earthquake response analysis is presented to demonstrate that the stacks can sustain significant inelastic deformations without collapse. A significant part of seismic input energy is dissipated through hysteretic action, and therefore, stacks could be designed for ductile behavior.

INTRODUTION

Reliable design of stack-like structures, e.g., intake-outlet towers, chimneys, etc., located in highly seismic areas requires the determination of their capacity to resist the dynamic forces induced by intense ground motions. For such intense motions, that may occur rarely during the life of the structure, significant inelastic behaviour (and limited damage) is generally anticipated and safety of these structures is ensured by providing sufficient ductility. Frequently, however, codes are not explicit about the interaction between design elastic strength and actual ductility capacity.

Lack of research on the nonlinear response of reinforced concrete stack-like structures, and on the collapse threshold for such structures subjected to ground shaking precludes reliable evaluation of their ductile behaviour. For many years, it has been assumed that in stack-like structures, it would be difficult to develop lateral displacement ductility in excess of two (Newmark and Rosenblueth, 1971, Chopra and Liaw, 1975) because extensive yielding of one section may lead to extensive displacements or collapse. Very slender stacks may be specially vulnerable because of the importance of gravity effects. Therefore, most of the design standards (ACI 307-79) specify increased design earthquake force-level for stack-like structures than those for buildings, basically not to impose large ductility requirements on such structures.

---

* Formerly Post-Graduate Student
** Associate Professor

However, dynamic stability of properly detailed stacks in the inelastic range, even after extensive yielding of one section, can not be ruled out because earthquake ground motion acts for a very short duration and rapidly changes direction several times. Consequently, the actual earthquake resistance of the stacks may be significantly more than what is estimated from the existing methods using elastic dynamic analysis. It is, therefore, necessary to develop a better understanding of the inelastic (ductile) behaviour and actual seismic resistance of reinforced concrete stacks.

In earlier investigations on inelastic response of reinforced concrete stacks, a bilinear elasto-plastic stress-strain relation, with equal yield strength in tension and compression, was assumed for the equivalent homogeneous material (Shiau and Yang, 1980). Additionally, the effects of geometric nonlinearity were not included in the analysis. The prediction of true collapse threshold of reinforced concrete stack-like structures under strong ground motions, however, requires a more rigorous formulation that can incorporate realistic material behavior and the effects of gravity. The objective of this investigation is therefore to develop reliable techniques for analyzing the inelastic dynamic response of reinforced concrete stack-like structures.

FINITE ELEMENT FORMULATION

System, Discretization and Coordinate System

The system considered consists of a tapered reinforced concrete stack with hollow circular cross-section fixed at the base. The stack cross-sections are provided with two rings of longitudinal reinforcements and cages of circumferential reinforcement placed near both the inside and outside faces of the section (Fig. 1). It is assumed that the bar sizes and spacing of circumferential steel, selected in detailing, are appropriate 1) to prevent premature buckling of the longitudinal reinforcement, and 2) to provide sufficient shear resistance so that the collapse of the stack is due to crushing of concrete in primary stress arising from axial load and flexure. The stack is analyzed for the single horizontal component of the free-field ground acceleration, and therefore, only planer vibrations of the stack are considered in this investigation.

An incremental step-by-step finite element procedure is followed for the nonlinear analysis, in which solution is obtained at closely spaced discrete time steps. The deformed configuration of the stack is idealized as an assemblage of beam elements (Fig. 2). Sufficient number of beam elements are used so that the rotations relative to the chord of the deformed element are small. This allows the idealization of the curved deformed beam element by the straight chord passing through the current positions of the two end nodes. The stack as a whole can undergo large deflection and large rotation but small strain. For each beam element, a local coordinate system x-y passing through the two end nodes, is defined (Fig. 2). The origin and direction of this coordinate system are continuously updated according to the current positions of the two end nodes. Thus rigid body motions are eliminated and the assumption of small displacement theory remains valid when the incremental displacements of the element for the next load step are referred to this local coordinate system. Equilibrium equations for each element are written in the local coordinate system and then transformed to the fixed global X-Y coordinate system by using transformation matrices that are continuously updated.

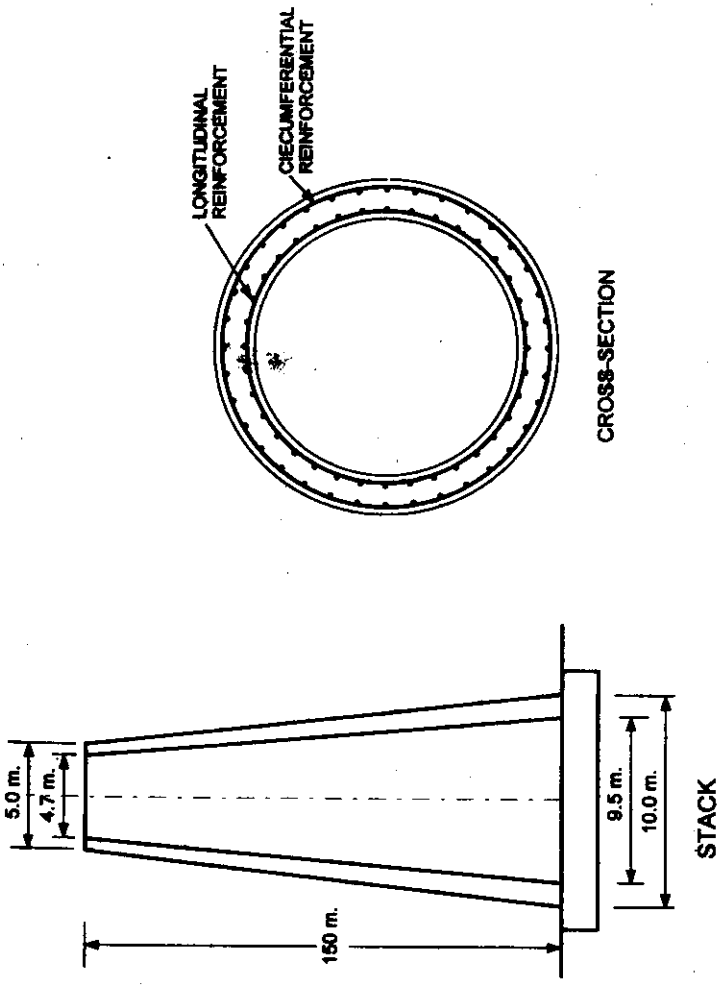

Figure 1. Typical reinforced concrete stack-like structure

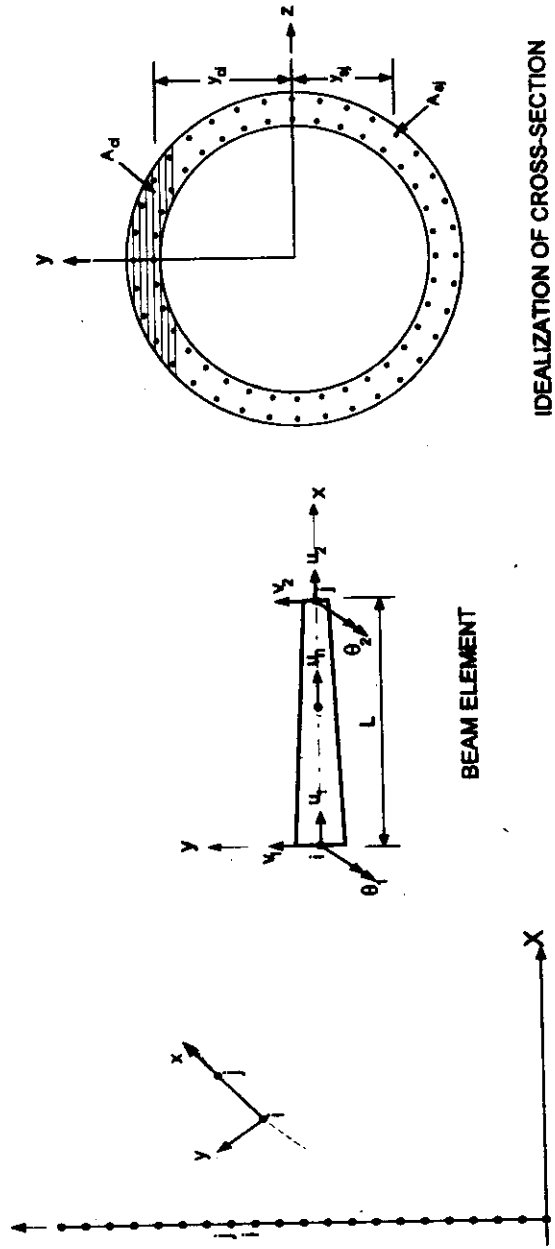

Figure 2. Finite element model of stack-like structure

Displacement and Strain Fields

The centroidal axis of the beam element has been selected as reference axis in the finite element formulation (Fig. 2). Axial displacement at the centroidal axis $u_0(x)$ is computed from the nodal displacements at beam ends, u_1 and u_2, using linear interpolation functions. Because of cracking and material nonlinearity, neutral axis may not coincide with the reference axis, and therefore, an additional incompatible axial degree of freedom, u_n, at the mid point of the element is considered to allow linear variation of axial strain along the reference axis (Chan, 1982). This incompatible degree of freedom is, however, condensed out at the element level. This leads to:

$$u_0 = \begin{bmatrix} \psi_1 & \psi_2 & \psi_n \end{bmatrix} \begin{Bmatrix} u_1 \\ u_2 \\ u_n \end{Bmatrix} \tag{1}$$

where

$$\psi_1 = 1 - \frac{x}{L}\,; \qquad \psi_2 = \frac{x}{L}\,; \qquad \psi_n = \frac{4x}{L}\left(1 - \frac{x}{L}\right) \tag{2}$$

in which L is the length of the element. The transverse displacement of the reference axis is computed from the nodal displacements in the transverse direction, v_1 and v_2, and rotations θ_1 and θ_2 at the beam ends, using standard cubic Hermitian interpolation functions (Bathe and Bolourchi, 1979), i.e.,

$$v_0 = \begin{bmatrix} \phi_1 & \phi_2 & \phi_3 & \phi_4 \end{bmatrix} \begin{Bmatrix} v_1 \\ v_2 \\ \theta_1 \\ \theta_2 \end{Bmatrix} \tag{3}$$

where

$$\phi_1 = 1 + 2\left(\frac{x}{L}\right)^3 - 3\left(\frac{x}{L}\right)^2\,; \qquad \phi_2 = 3\left(\frac{x}{L}\right)^2 - 2\left(\frac{x}{L}\right)^3 \tag{4a}$$

$$\phi_3 = L\left[\frac{x}{L} - 2\left(\frac{x}{L}\right)^2 + \left(\frac{x}{L}\right)^3\right]; \qquad \phi_4 = -L\left[\left(\frac{x}{L}\right)^2 - \left(\frac{x}{L}\right)^3\right] \tag{4b}$$

The axial displacement $u(x,y)$ and transverse displacement $v(x,y)$ at any point within the beam element are obtained by Euler Bernoulli's beam kinematics, i.e.,

$$u = u_0 - y\frac{dv_0}{dx} \tag{5}$$

$$v = v_0 \tag{6}$$

where u_0, v_0 are the displacements of the centroidal axis along x and y axes, respectively. The axial strain, ε, at any point is then expressed as:

$$\varepsilon = [\frac{du_0}{dx} - y\frac{d^2v_0}{dx^2}] + [\frac{1}{2}(\frac{dv_0}{dx})^2] \tag{7}$$

$$= [\varepsilon_l] + [\varepsilon_{nl}]$$

In this equation ε_l and ε_{nl} are linear and nonlinear components of the strain, respectively.

For evaluating the element matrices the cross-section is discretized into a number of strips parallel to the neutral axis (Fig. 2). For each strip of concrete, stress at any instant of time is computed according to the strain at the centroid of the strip using the cyclic stress-strain relationship of concrete. Similarly, each reinforcing bar is idealized independently and the stress in each reinforcing bar is computed according to the strain at its centroid using the cyclic stress-strain curve for reinforcing steel. The stress-strain relations of concrete and reinforcing steel used in this study are presented next.

Stress-Strain Relationship of Concrete

The mathematical model for cyclic stress-strain relationship of concrete, used in this study, is shown in Fig. 3. The envelope of the cyclic stress-strain curves in compression is represented by the curve obtained by monotonically increasing the load. The envelope curve consists of a second degree parabola for the ascending branch and a linear softening branch (Park and Ruitong, 1988). The parabolic part is represented by

$$\sigma_c = \sigma_{cy}\left[\frac{2\varepsilon_c}{\varepsilon_{cy}} - \left(\frac{\varepsilon_c}{\varepsilon_{cy}}\right)^2\right] \tag{8}$$

where σ_c and ε_c are concrete stress and strain respectively, σ_{cy} is the compressive strength of concrete, and ε_{cy}=0.002 is the strain at maximum stress. The linear softening branch is defined by an ultimate compressive strain ε_{cu} and a corresponding stress of $0.2\sigma_{cy}$. Concrete is assumed to have no tensile strength.

The cyclic unloading-reloading relation is assumed to be linear. If the maximum imposed strain in concrete is less than ε_{cy}, the slope of the unloading-reloading path is equal to the initial tangent modulus of elasticity E_c. If the maximum imposed compressive strain in concrete is greater than ε_{cy}, the slope of the unloading-reloading path is equal to E_cF_c, where F_c is given by (Blakely and Park, 1973) :

$$F_c = 0.8 - \frac{0.7(\varepsilon_{cm} - \varepsilon_{cy})}{\varepsilon_{cu} - \varepsilon_{cy}} \tag{9}$$

in which ε_{cm} is the maximum compressive strain attained. The reduction factor F_c takes into account the degradation of stiffness for both unloading and reloading curves for increasing values of maximum strain.

Stress-strain Relationship of Steel

The stress-strain relations of reinforcing steel, used in this study, is assumed as a bilinear stress-strain envelope and linear unloading-reloading behaviour upon stress reversal (Fig. 3). Stress-strain relation of reinforcing steel is assumed to be same in both tension and

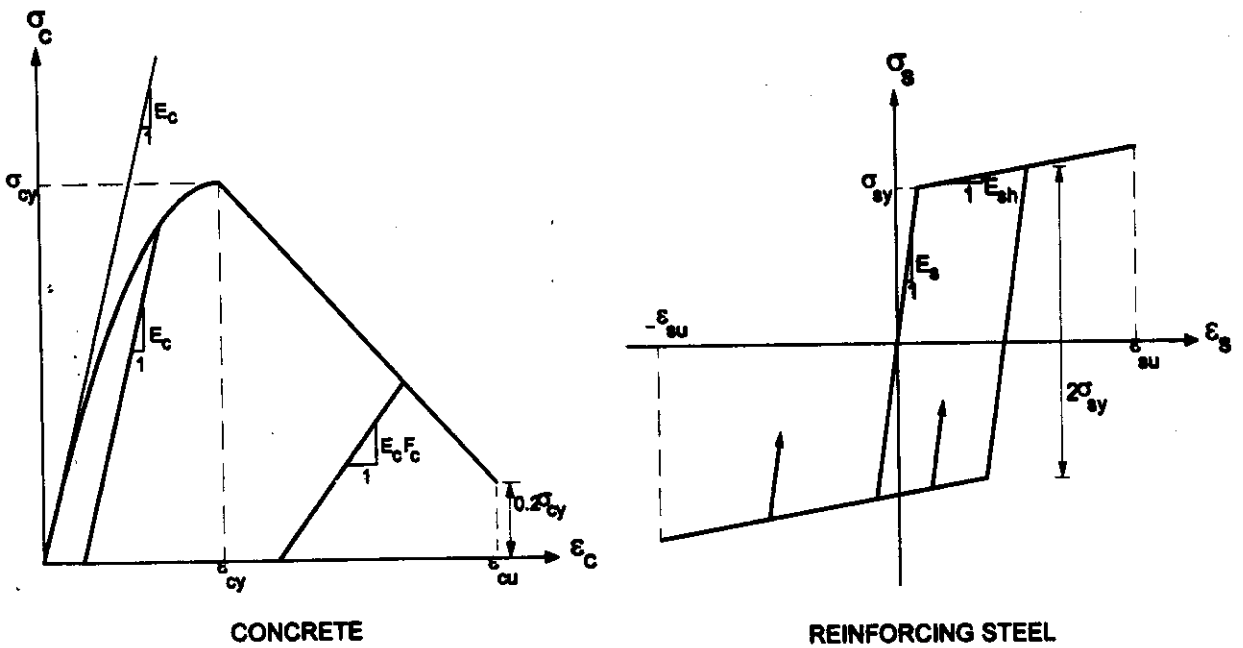

Figure 3. Stress-strain relationships for concrete and reinforcing steel

compression. The slope of the unloading-reloading branch is same as the initial elastic modulus of steel. The reinforcing steel is assumed to fail when the strain in any direction exceeds the ultimate strain ε_{su}. The complete stress-strain behaviour is defined by four parameters: initial modulus of elasticity E_s, strain hardening modulus E_{sh}, yield stress σ_{sy}, and ultimate strain ε_{su}.

Equations of Motion

Knowing the solution at time t, the incremental equilibrium equations of motion at time $t+\Delta t$ are obtained from the principle of virtual work. Let $\Delta\sigma$ and $\Delta\varepsilon$ be the increments in stress and strain, respectively, from time t to $t+\Delta t$. Expressing the strain increment $\Delta\varepsilon$ as a sum of linear and nonlinear components of strain ($\Delta\varepsilon_l + \Delta\varepsilon_{nl}$), the linearized equations of motion are (Bathe, 1982):

$$\sum_e \int_{V^e} \Delta\varepsilon_l \, E_t \, \delta\Delta\varepsilon_l \, dV^e + \sum_e \int_{V^e} \sigma \, \delta\Delta\varepsilon_{nl} \, dV^e = \sum_e \int_{V^e} -[\ddot{u}^{tot}_{t+\Delta t} \quad \ddot{v}^{tot}_{t+\Delta t}] \rho \begin{Bmatrix} \delta\Delta u \\ \delta\Delta v \end{Bmatrix} dV^e + \sum_e \int_{V^e} \rho g [-n_x \quad -n_y] \begin{Bmatrix} \delta\Delta u \\ \delta\Delta v \end{Bmatrix} dV^e - \sum_e \int_{V^e} \sigma \, \delta\Delta\varepsilon_l \, dV^e \tag{10}$$

where the summation sign indicates sum over all the elements. In equation (10), E_t is the tangent modulus of elasticity for uniaxial state of stress of the infinitesimal volume element at time t; $\ddot{u}^{tot}_{t+\Delta t}$ and $\ddot{v}^{tot}_{t+\Delta t}$ are the total accelerations of the volume element at time $t+\Delta t$ in the local x and y directions, respectively; $\delta\Delta u$ and $\delta\Delta v$ are the corresponding virtual displacements; $\delta\Delta\varepsilon$ is the virtual strain; ρ is the mass density of the stack material; g is the acceleration due to gravity; and n_x and n_y are the direction cosines of the local x axis with respect to global X and Y axes.

The incremental displacement field within the beam element is expressed as a function of the nodal displacement increments using the displacement interpolation functions [equations (1) and (3)]. Substituting the displacement and strain interpolation functions, equation (10) can be expressed in terms of the nodal displacement increments:

$$\sum_e (\mathbf{k}_e)_t \Delta\mathbf{v}^e_t + \sum_e (\mathbf{k}_g)_t \Delta\mathbf{v}^e_t = \sum_e -\mathbf{m}_t \ddot{\mathbf{v}}^{e(tot)}_{t+\Delta t} + \sum_e \mathbf{r}^g_t - \sum_e \mathbf{f}_t \tag{11}$$

where $\mathbf{m}_t$ is the element mass matrix, $(\mathbf{k}_e)_t$ is the element elastic stiffness matrix after eliminating the incompatible axial degree of freedom u_n by static condensation, and $(\mathbf{k}_g)_t$ is the element geometric stiffness matrix, all defined in the element local coordinate system at time t. In this equation, $\Delta\mathbf{v}^e_t$ is vector of incremental displacements at the element nodal degrees of freedom; $\ddot{\mathbf{v}}^{e(tot)}_{t+\Delta t}$ is the vector of total accelerations at the element nodal degrees of freedom; and $\mathbf{r}^g_t$ is the equivalent nodal load vector at time t due to gravity. In evaluating the element matrices, numerical integration over the length of the element is performed by Gauss quadrature, and over the cross-section at each Gauss point by layer integration.

The equilibrium equation of the entire structure is obtained by the standard direct stiffness assembly process. Before the element matrices are assembled, they are transformed to fixed global coordinate system using the updated transformation matrices. The assembled,

linearized, incremental equations of equilibrium, including the damping term, for planar vibrations of stack subjected to ground motion $\ddot{u}_g$ at time $t+\Delta t$, where Δt is the increment in time, are:

$$(\mathbf{K}_e)_t \Delta \mathbf{v}_t + (\mathbf{K}_g)_t \Delta \mathbf{v}_t = -\mathbf{M}_t(\mathbf{1}_x[\ddot{u}_g]_{t+\Delta t} + \ddot{\mathbf{v}}_{t+\Delta t}) + \mathbf{R}_t^g - \mathbf{F}_t - \mathbf{C}_t \dot{\mathbf{v}}_{t+\Delta t} \qquad (12)$$

in which $\mathbf{M}_t$ is the structure mass matrix, $(\mathbf{K}_e)_t$ is the structure elastic stiffness matrix and $(\mathbf{K}_g)_t$ is the structure geometric stiffness matrix, all defined in a fixed global coordinate system for known equilibrium configuration at time t; $\ddot{\mathbf{v}}_{t+\Delta t}$ and $\dot{\mathbf{v}}_{t+\Delta t}$ are the vectors of relative velocity and acceleration, respectively, at time $t+\Delta t$; $\mathbf{1}_x$ is the vector of ones and zeros identifying the degrees of freedom in the direction of ground acceleration $[\ddot{u}_g]_{t+\Delta t}$; $\mathbf{R}_t^g$ is the equivalent nodal load vector due to gravity for the entire structure at time t ; and $\mathbf{C}_t$ is the structure damping matrix. In this formulation, an instantaneous Rayleigh damping matrix is used to give the specified damping in the first two modes throughout the time history analysis, i.e.,

$$\mathbf{C}_t = a_t \mathbf{M}_t + b_t (\mathbf{K}_e)_t \qquad (13)$$

The coefficients, a_t and b_t, are computed from the tangent frequencies in the first two modes. It may be noted that the mass matrices of the elements in their local coordinate axes remain constant but the transformation matrices from local to global coordinates change due to change in geometry of the structure. Therefore, the global mass matrix changes with time.

Equation (12) can be solved by time integration procedure for the incremental displacements, velocities and accelerations. However, the values obtained for displacements, velocities and accelerations at time $t+\Delta t$ by adding these increments to known values of displacements, velocities and accelerations, respectively, at time t, may not satisfy the exact equations of equilibrium at time $t+\Delta t$. Therefore, iterations are performed within each time step so that equilibrium is satisfied at time $t+\Delta t$.

Response Quantities

Once the nodal displacement increments are known, strain increment at any point within the element is obtained from the strain displacement relations [equation (7)]. The incremental strains are added to the strains at time t to obtain the current state of strain. From these strains, stresses are calculated from appropriate stress-strain curves. Bending moment, $\mathcal{M}$, at each Gauss point is computed by taking moment of the forces in the concrete layers and reinforcing steel bars about the centroidal axis of the section as:

$$\mathcal{M} = \int_A y\sigma \, dA = \sum_{i=1}^{N_c} y_{ci} \, A_{ci} \, \sigma_{ci} + \sum_{j=1}^{N_s} y_{sj} \, A_{sj} \, \sigma_{sj} \qquad (14)$$

where A_{ci} is the area of concrete layer i; y_{ci} is the distance of concrete layer i from the centroidal axis of the section; σ_{ci} is the stress in concrete at the centroid of concrete layer i; A_{sj} is the area of steel bar j; y_{sj} is the distance of the center of the steel bar j from the centroidal axis of the section; and σ_{sj} is stress in steel bar j. N_c and N_s are the total number of concrete layers and steel bars, respectively. Equivalent moments at the two ends of an

element are used to compute the constant shear force in that element. Axial force at Gauss point is computed by adding the forces in concrete layers and reinforcing bars as:

$$P = \int_A \sigma \, dA = \sum_{i=1}^{N_c} A_{ci} \sigma_{ci} + \sum_{j=1}^{N_s} A_{sj} \sigma_{sj} \tag{15}$$

Axial force in any element is taken as the average of the axial forces at the Gauss points.

Seismic Energy Computation

The absolute energy formulation (Uang and Bertero, 1990) has been used to derive the energy balance equation:

$$E_i = E_k + E_\zeta + E_a \tag{16}$$

The left and right hand side terms of equation (16) are computed independently to ensure the correctness of the solution. The total seismic input energy, E_i, in equation (16) is computed as:

$$E_i = \int (\ddot{\mathbf{v}}_t^{tot})^T \mathbf{M}_t \, d\mathbf{v}_g \tag{17}$$

in which $\ddot{\mathbf{v}}_t^{tot}$ is the total acceleration vector at time t, and $\mathbf{v}_g$ is a vector defined by $\mathbf{1}_x v_g$, where v_g is the ground displacement at time t, and $\mathbf{1}_X$ is the vector of ones and zeros identifying the degrees of freedom in the direction of ground acceleration. The first term on the right hand side in equation (16) represents the total kinetic energy, E_k,

$$E_k = \int (\dot{\mathbf{v}}_t^{tot})^T \mathbf{M}_t \dot{\mathbf{v}}_t^{tot} \, dt \tag{18}$$

The second term represents the damping energy, E_ζ,

$$E_\zeta = \int \dot{\mathbf{v}}_t^T \mathbf{C}_t \dot{\mathbf{v}}_t \, dt \tag{19}$$

The third term represents the total deformation energy, E_a, including both recoverable elastic energy, E_r, and the non-recoverable hysteretic energy, E_h :

$$E_a = E_r + E_h = \int (\mathbf{F}_t - \mathbf{R}_t^g)^T \, d\mathbf{v} \tag{20}$$

The work done by the gravity forces during earthquake excitation is not included in this expression of total deformation energy.

The recoverable elastic energy, E_r, at any instant of time is estimated by

$$E_r = \sum_e \int_{V^e} \frac{(\sigma - \sigma_0)^2}{2E_t} \, dV^e \tag{21}$$

where σ is the stress at the infinitesimal volume element at time t; σ_0 is the initial stress due to self weight of stack; and E_t is the modulus of elasticity of material at time t. This estimate

of recoverable elastic energy in the presence of initial stress is valid when the modulus of elasticity in unloading does not change with time. Since slope of the unloading branch of concrete changes after the compressive strain exceeds ε_{cy}, the above estimate may be in little error when concrete strain is more than ε_{cy}. Additionally, the contribution of the gravity effects in the recoverable energy is small and therefore not deducted while deriving the expression for the recoverable elastic energy, E_r, in the present study. The estimates of hysteretic energy dissipation, $E_h = E_a - E_r$, therefore will not have significant errors because recoverable elastic energy is negligible in comparison to the non-recoverable hysteretic energy after the strong excitation phase of the ground motion.

SOLUTION PROCEDURE

Direct Time Integration With Equilibrium Iteration

The linearized equation of motion at time $t+\Delta t$ [equation (12)] is solved by direct time integration using Newmark's average acceleration scheme in which the incremental velocities and accelerations from time t to $t+\Delta t$ can be expressed in terms of the displacement increments over the same time interval:

$$\Delta\ddot{\mathbf{v}}_t = \frac{1}{\Delta t^2\beta}\Delta\mathbf{v}_t - \frac{1}{\Delta t\beta}\dot{\mathbf{v}}_t - \frac{1}{2\beta}\ddot{\mathbf{v}}_t;\ \Delta\dot{\mathbf{v}}_t = \frac{\gamma}{\Delta t\beta}\Delta\mathbf{v}_t - \frac{\gamma}{\beta}\dot{\mathbf{v}}_t + \Delta t[1-\frac{\gamma}{2\beta}]\ddot{\mathbf{v}}_t \tag{22}$$

where $\beta = 1/4$ and $\gamma = 1/2$. Because of the linearization of the exact equation of motion, equilibrium iterations are performed within each time step using Newton-Raphson's scheme. The governing equation for the $(l+1)$st iteration within a time step is (Bathe, 1982):

$$\begin{aligned}&[(\mathbf{K}_e)_t^l + (\mathbf{K}_g)_t^l + \frac{1}{\Delta t^2\beta}\mathbf{M}_t + \frac{\gamma}{\Delta t\beta}\mathbf{C}_t]\delta\mathbf{v}^{l+1} = -\mathbf{M}_t\mathbf{1}_x[\ddot{u}_g]_{t+\Delta t} + \mathbf{R}_t^{s^l} - \mathbf{F}_t^l - \\ &\mathbf{M}_t[\frac{1}{\Delta t^2\beta}\Delta\mathbf{v}_t^l - \frac{1}{\Delta t\beta}\dot{\mathbf{v}}_t - (\frac{1}{2\beta}-1)\ddot{\mathbf{v}}_t] - \mathbf{C}_t[\frac{\gamma}{\Delta t\beta}\Delta\mathbf{v}_t^l - (\frac{\gamma}{\beta}-1)\dot{\mathbf{v}}_t + \Delta t(1-\frac{\gamma}{2\beta})\ddot{\mathbf{v}}_t]\end{aligned} \tag{23}$$

where

$$\Delta\mathbf{v}_t^l = \Delta\mathbf{v}_t^{l-1} + \delta\mathbf{v}^l \tag{24}$$

The superscript l indicates that the quantities are evaluated for the displacement $(\mathbf{v}_t + \Delta\mathbf{v}_t^l)$. Mass and damping matrices at the beginning of a time step are kept constant for all the iterations within that time step.

After each iteration the solution is checked for convergence with respect to prescribed tolerances on the unbalanced forces, the incremental displacements, and the incremental energy. The following convergence criteria are used in the present study (Bathe, 1982):

$$\frac{\|\Delta\mathbf{F}^{l+1}\|_2}{\|\Delta\mathbf{F}^0\|_2} < f_{tol};\qquad \frac{\|\delta\mathbf{v}^{l+1}\|_2}{\|\mathbf{v}_t + \Delta\mathbf{v}_t^{l+1}\|_2} < d_{tol};\qquad \frac{[\Delta\mathbf{F}^l]^T\delta\mathbf{v}^{l+1}}{[\Delta\mathbf{F}^0]^T\delta\mathbf{v}^1} < e_{tol} \tag{25}$$

where ΔF^{i+1} is the unbalanced effective force vector after $(i+1)$st iteration, and $\| \ \|_2$ denotes Euclidean vector norm. The convergence limits f_{tol} and d_{tol} are taken as 10^{-4} and 10^{-3}, respectively, and the energy tolerance, e_{tol}, is taken as 10^{-7}, i.e., the product of f_{tol} and d_{tol}.

Adaptive Reduction of Time Step

In nonlinear earthquake analysis of reinforced concrete stacks, main sources of nonlinearity are cracking of concrete, yielding of reinforcing steel and nonlinear stress-strain curve of concrete with strain softening at higher strain. Large time steps in the numerical integration scheme sometimes lead to instability of the solution. Therefore, to ensure convergence to right solution, a typical reinforced concrete stack (Fig. 1) is analyzed repeatedly for S69E component of Taft earthquake (1952), scaled up to a peak acceleration of 1.8g, with reducing time steps of integration. It was observed that a very small time-step, i.e., 0.0005 sec., needs to be used in numerical integration scheme for this stack to achieve convergence of all response quantities.

The envelope values for lateral displacements, shear forces and bending moments along the height of the stack, obtained with integration time steps of 0.0005 sec., are presented in Fig. 4. However, using such a small time-step throughout the ground excitation record requires prohibitive computational efforts. Therefore, an adaptive time-step reduction procedure is proposed in which a large time-step is used initially, and whenever displacements or forces change rapidly, time-step is adaptively reduced.

In this adaptive time-step reduction procedure, the time step is halved when strain increment in any strip, or in a reinforcing bar, at any of the Gauss points exceeds twenty-five percent of the yield strain of reinforcing steel, or when the incremental moment at any Gauss point exceeds five percent of the moment capacity at that section. The limit on the strain increment ensures a smooth change in equilibrium configuration. The limit on the incremental moment restricts rapid change in forces due to closing of cracks or unloading in any step. Apart from these two limits, the time-step is halved if convergence is not achieved after four iterations for equilibrium in a time-step. Whenever the normal time-step is reduced, the next incremental time-step is adjusted to complete the normal time-step so that the subsequent integration could be continued with normal time-step. The response results obtained using a normal time-step of 0.02 second with adaptive time-step reduction, and those that are obtained with a constant time-step of 0.0005 second, have been compared in Fig. 4. The response results in these two cases are in excellent match, whereas the computational effort required in the proposed method is one eighth of that required with the constant time-step of 0.0005 sec.

NONLINEAR RESPONSE : NUMERICAL EXAMPLE

The developed procedure is utilized to obtain the nonlinear earthquake response of a typical, linearly tapered, reinforced concrete stack (Fig. 1). The mass density of the stack shell is assumed as 3000 N-s^2/m^4 to give the axial force ratio $P/A_g\sigma_{cy} = 0.2$ at the base, where P is the axial force at base, A_g is the area of cross section at base, and σ_{cy} is the maximum compressive stress of concrete. The maximum compressive stress, σ_{cy}, and the ultimate compressive strain, ε_{cu}, of concrete are taken as 13.33 MPa and 0.005, respectively.

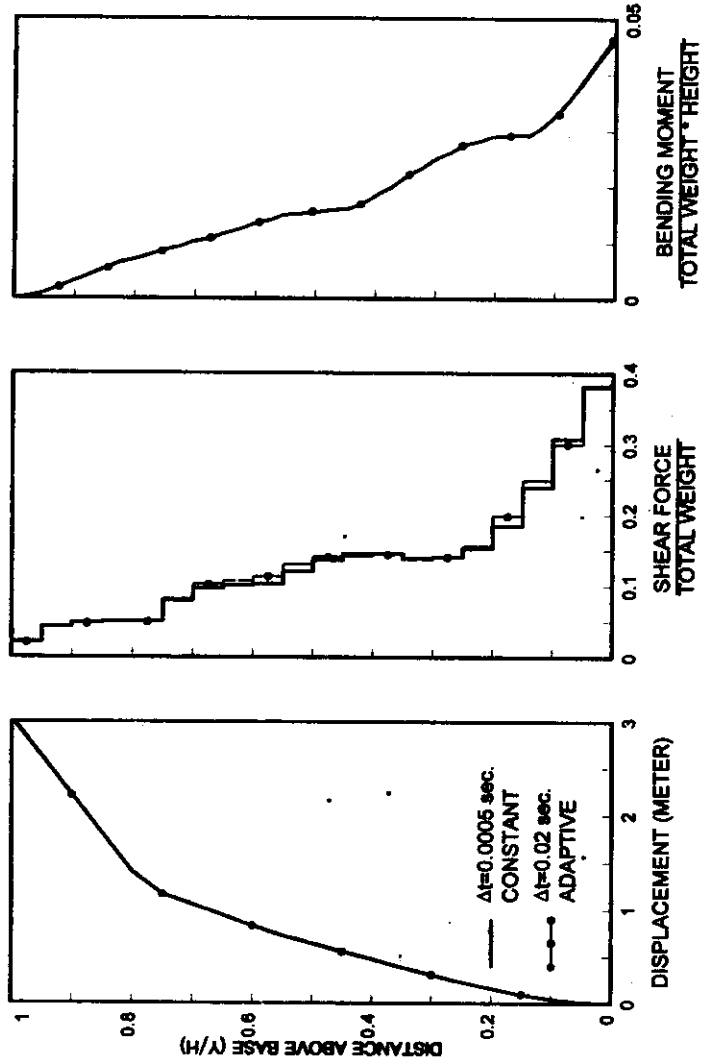

Figure 4. Envelopes of lateral displacement, shear force and bending moment in the stack with (1) constant time step of 0.0005 sec., and (2) time step of 0.02 sec. with adaptive reduction

The parameters defining the stress-strain curve of reinforcing steel are taken as: $\sigma_{sy} = 380$ MPa, $E_s = 2 \times 10^5$ MPa, $E_{sh} = E_s / 200$, and $\varepsilon_{su} = 0$.

The stack is discretized into 20 equal beam elements and in each element, three Gauss points are considered for numerical integration along the length of the element. At each gauss point the cross section is divided into 72 strips (Fig. 2). Two hundred individual reinforcing bars are considered in each of the two longitudinal reinforcing steel layers to give the reinforcing steel area equal to 0.5 percent of the area of concrete. The normal time-step of integration is taken as Δt=0.02 second, which is about 1/220 of the fundamental time period of the initial unloaded structure, with adaptive reduction of time-step as mentioned earlier. An instantaneous damping matrix is used to give three percent damping in the first two modes. A single horizontal component of Taft ground motion (S69E), scaled-up to 1.8g peak ground acceleration, is used in this study. Although this highly intense ground motion is very unlikely to occur anywhere, the same is used here to ensure that the stack goes into considerable inelastic range.

The stack is analyzed for the scaled up Taft ground motion assuming both material and geometric nonlinearities, and the response results are compared with those obtained from linear elastic analysis for the same ground motion. In the linear elastic analysis, the modulus of elasticity of concrete and that of steel are taken as the initial values in their corresponding stress-strain curves.

The results of the computer analysis consist of the response histories of displacements at nodal points and shear forces, bending moments and axial forces at the Gauss points along the height of the stack. Additionally, the time histories of total input energy, total dissipated energy, damping energy and hysteretic energy for the stack are obtained. Only a small portion of the response results is presented in Figs. 5 and 6 for the example stack. Envelope values of lateral displacements, shear forces and bending moments along the height from linear and nonlinear analyses are presented in Fig. 5, and various energy time histories are presented in Fig. 6. The displacement envelopes obtained from the two analyses are almost similar upto the height where maximum yielding occurs in the nonlinear case. Above this level, displacements in the nonlinear case are more apparently because of large rotation at the point of maximum yielding. As anticipated, maximum bending moment and shear force over the height are much less in the nonlinear case because maximum bending moment permitted in nonlinear case is the strength of the structure in bending. The actual bending strength of the section along the height of the stack, computed from the yield stress of steel and maximum compressive stress of concrete, is also shown in Fig. 5 that also demonstrates that the section capacity has been reached at the point of maximum yielding.

The seismic input energy dissipation in the nonlinear analysis is accounted for by both viscous damping mechanisms, and the hysteretic action. The time histories of total input energy, total dissipated energy, damping energy and hysteretic energy for the nonlinear case have been shown in Fig. 6. As it is demonstrated, a significant part of seismic input energy is dissipated through hysteretic action.

In order to understand why the stack remains stable even after significant yielding of one cross-section, the displaced shapes of the stack at different instants of time (when maximum top displacement occurs) have been plotted in Fig. 7 along with ground displacement at each instant. It is demonstrated in this Figure that the stack does not move in

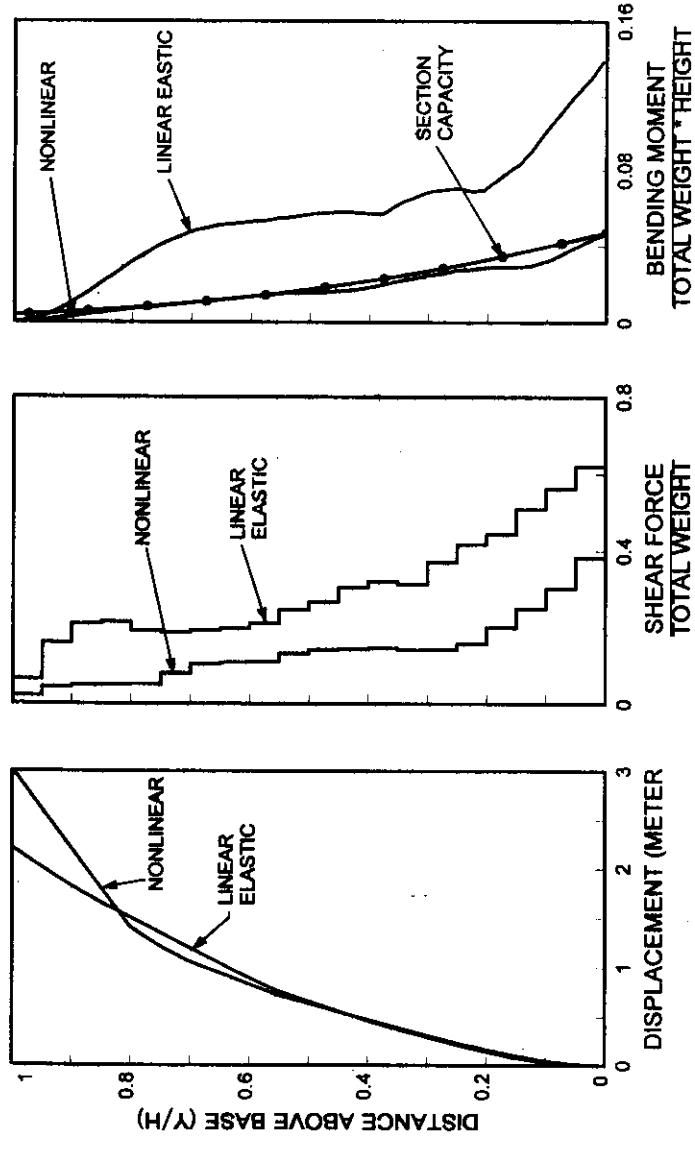

Figure 5. Comparison of envelope values of lateral displacement, shear force and bending moment in nonlinear and linear elastic analyses

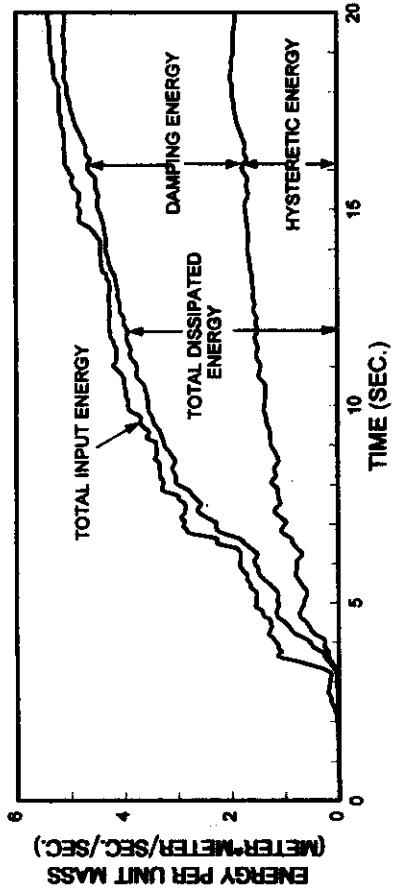

Figure 6. Energy time-histories in nonlinear analysis

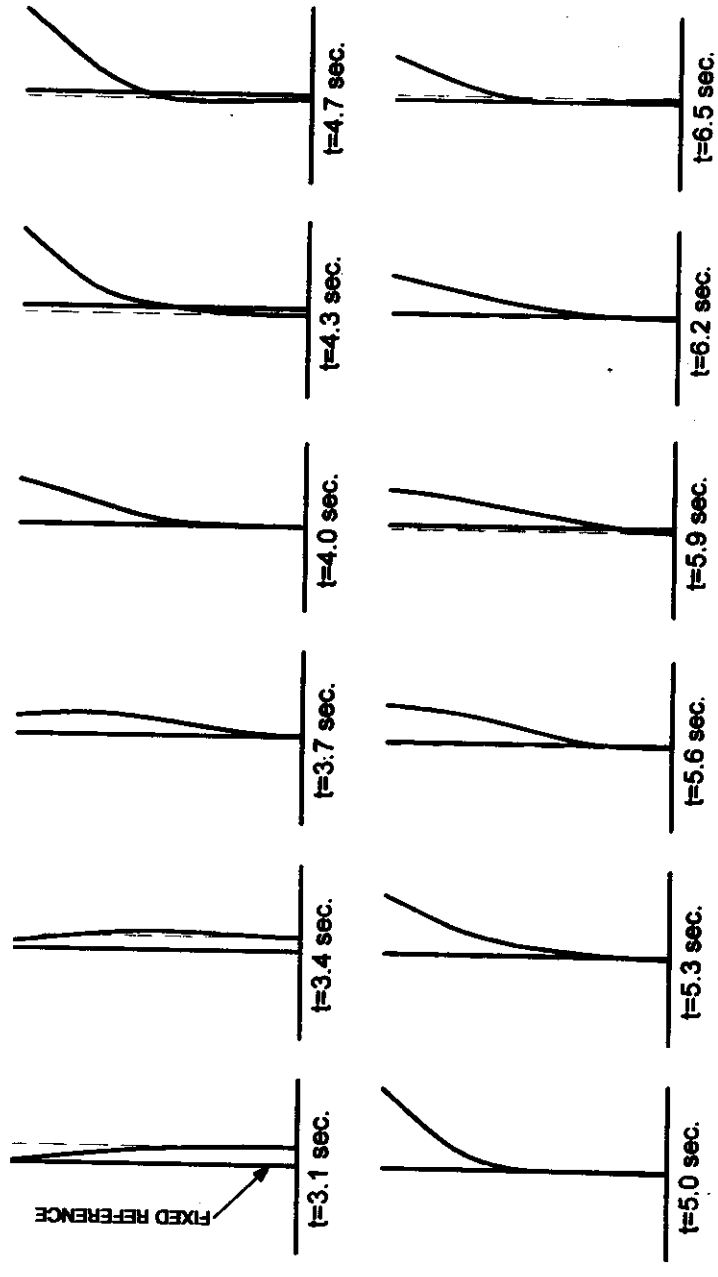

Figure 7. Deformed shapes of the stack at various instants of time in nonlinear analysis

a single direction to total collapse due to reversal of the direction of ground motion. Specifically, when the maximum top displacement is reached, direction of the ground displacement reverses and the stack is forced to move in the opposite direction, thus preventing collapse. It can therefore be concluded that for this example stack and ground motion, even after significant yielding of one section, displacements and self weight are not large enough to cause failure due to gravity effects because earthquake forces are of short duration and reversible in nature.

CONCLUSIONS

A reliable and efficient technique for analyzing the inelastic response of reinforced concrete stack-like structures has been presented. The finite element formulation presented in this paper is based on the actual stress-strain relationships for concrete and reinforcing steel. The overall efficiency of the analysis procedure lies in using the adaptive reduction of integration time-step in the numerical scheme.

It has been demonstrated that a reinforced-concrete stack can sustain a severely strong earthquake without total collapse if it is permitted to undergo inelastic deformations. The stack remains stable even after significant yielding of one section as earthquake forces are for short duration and reversible in nature. Because a significant part of seismic input energy can be dissipated by hysteretic action, the stack can be designed for the ductile response.

APPENDIX I : NOTATIONS

a_t time-dependent coefficient of mass matrix in Rayleigh damping matrix

b_t time-dependent coefficient of stiffness matrix in Rayleigh damping matrix

$\mathbf{C}_t$ structure damping matrix at time t

E_a deformation energy

E_c modulus of elasticity of concrete

E_h hysteretic energy dissipation

E_i seismic input energy

E_k kinetic energy

E_r recoverable elastic energy

E_s modulus of elasticity of reinforcing steel

E_{sh} straining hardening modulus of reinforcing steel

E_t tangent elastic modulus of material

E_ξ damping energy

F_c modulus of elasticity factor for concrete

$\mathbf{F}_t$ internal resisting force vector at time t

$\mathbf{k}_e$ element elastic stiffness matrix

$\mathbf{k}_g$ element geometric stiffness matrix

$\mathbf{K}_t$ structure stiffness matrix at time t

L length of beam element

$\mathbf{m}$	element mass matrix
$\mathbf{M}$	structure mass matrix
m	bending moment at Gauss point
P	axial force on a section
$\mathbf{r}^g$	equivalent nodal load vector due to gravity in an element
$\mathbf{R}^g$	equivalent nodal load vector due to gravity
Δt	incremental time step
u	displacement in the local x direction at any point on the beam element
u_0	displacement in the local x direction at any point on the reference axis
v_0	displacement in the local y direction
$\mathbf{v}^e$	element nodal displacement vector
$\mathbf{v}$	global displacement vector
$\dot{\mathbf{v}}$	global velocity vector
$\ddot{\mathbf{v}}$	global acceleration vector
$\Delta\mathbf{v}_t$	incremental displacement vector from time t to $t + \Delta t$
$\Delta\dot{\mathbf{v}}_t$	incremental velocity vector from time t to $t + \Delta t$
$\Delta\ddot{\mathbf{v}}_t$	incremental acceleration vector from time t to $t + \Delta t$
β	parameter in direct time integration
ε_c	strain in concrete
ε_{cy}	strain in concrete at maximum compressive stress
ε_l	linear component of the strain
ε_{nl}	nonlinear component of the strain
ε_{su}	ultimate strain of reinforcing steel
$\Delta\varepsilon$	incremental strain
γ	parameter in direct time integration
σ	stress at any point on the element
σ_c	stress in concrete
σ_{cy}	maximum compressive stress in concrete
σ_{sy}	yield stress of reinforcing steel
$\Delta\sigma$	incremental stress

REFERENCES

1. N. M. Newmark and E. Rosenblueth (1971), "Fundamentals of Earthquake Engineering", Prentice-Hall, Englewood Cliffs, New Jersey.

2. A. K. Chopra and C.-Y. Liaw (1975), "Earthquake resistant design of intake-outlet towers", J. Struct. Div. ASCE 101, pp. 1349-1366.

3. ACI 307-79 (1979), "Specifications for Design and Construction of R.C. Chimneys", American Concrete Institute, Detroit.

4. L. C. Shiau and T. Y. Yang (1980), "Elastic plastic seismic-response of chimney", J. Struct. Div. ASCE 106, 791-807.

5. E. C. Chan (1982), "Nonlinear geometric, material and time dependent analysis of reinforced concrete shells with edge beams", Report No. UCB/SESM-82/08, University of California, Berkeley, California.

6. K. J. Bathe and S. Bolourchi (1979), "Large displacement analysis of three-dimensional beam structures", Int. Jour. Num. Methods Eng. 14, pp. 961-986.

7. R. Park and D. Ruitong (1988), "Ductility of doubly reinforced concrete beam sections", ACI Structural Journal, pp. 217-225.

8. R. W. G. Blakely and R. Park (1973), "Prestressed concrete sections with cyclic flexure", J. Struct. Div. ASCE 99, pp. 1717-1742.

9. K. J. Bathe (1982), "Finite Element Procedures in Engineering Analysis", Prentice-Hall, New Jersey.

10. C. M. Uang and V. V. Bertero (1990), "Evaluation of seismic energy in structures", Earthquake Eng. Struct. Dyn. 19, pp. 77-90.